

## **Distribution Agreement**

In presenting this thesis as a partial fulfillment of the requirements for a degree from Emory University, I hereby grant to Emory University and its agents the non-exclusive license to archive, make accessible, and display my thesis in whole or in part in all forms of media, now or hereafter now, including display on the World Wide Web. I understand that I may select some access restrictions as part of the online submission of this thesis. I retain all ownership rights to the copyright of the thesis. I also retain the right to use in future works (such as articles or books) all or part of this thesis.

Joshua Chiok

April 10, 2024

Identification of a Novel Phosphorylation Site on Alpha-Synuclein Within Erythrocyte Ghost  
Membranes

By

Joshua Chiok

Blaine Roberts, PhD.  
Advisor

Department of Neuroscience and Behavioral Biology

Blaine Roberts, PhD.

Advisor

Shaima Nazaar, PhD.

Committee Member

Marcela Benítez, PhD.

Committee Member

Matthew Weinschenk, PhD.

Committee Member

April 10, 2024

Identification of a Novel Phosphorylation Site on Alpha-Synuclein Within Erythrocyte Ghost  
Membranes

By

Joshua Chiok

Blaine Roberts, PhD.

Advisor

An abstract of  
a thesis submitted to the Faculty of Emory College of Arts and Sciences  
of Emory University in partial fulfillment  
of the requirements of the degree of  
Bachelor of Sciences with Honors

Neuroscience and Behavioral Biology

April 10, 2024

## Abstract

### Identification of a Novel Phosphorylation Site on Alpha-Synuclein Within Erythrocyte Ghost Membranes

By Joshua Chiok

**Background:** Parkinson's disease (PD) is the second most prevalent neurodegenerative disorder and is on the rise within the aging population of the United States. PD is typically detected during its advanced stages, when significant neuron degeneration has occurred. The challenge of diagnosing PD early is of the utmost importance, with significant implications for improving the overall quality of life of individuals living with the disease. A potential solution to achieving early PD diagnosis lies in the development of minimally invasive diagnostic biomarkers such as the detection of phosphorylated alpha-synuclein in RBCs utilizing mass spectrometry. The goal of this study is to discover novel phosphorylation sites in erythrocyte ghost membranes that can later be evaluated as potential biomarkers for diagnosing PD.

**Methods:** A pool of RBCs were obtained from The Australian Imaging, Biomarker & Lifestyle Flagship Study of Ageing (AIBL). Erythrocyte ghost membranes were extracted from the AIBL pool of RBCs and then underwent phosphoenrichment via immobilized metal affinity chromatography using the Agilent AssayMap Bravo platform. After phosphoenrichment, samples were placed in a Bruker timsTOF fleX coupled to a Bruker nanoElute2 nanoHPLC. Data was acquired using a default data dependent acquisition (DDA) method on MS. Data was analyzed using Skyline and FragPipe software.

**Results:** 0.5% glycolic acid in the binding buffer of Fe-NTA IMAC phosphoenrichment was optimal. 10% acetonitrile in the elution buffer of Fe-NTA IMAC phosphoenrichment was optimal. Fe-NTA IMAC had a greater percentage of unique phosphopeptides and contained our target protein alpha-synuclein in comparison to our TiO<sub>2</sub> OMAC phosphoenriched samples that did not contain alpha-synuclein. 100 µg of erythrocyte ghost membranes was the optimal sample load for MS analysis. Alpha-synuclein was found to be phosphorylated at Y125 and S129 as documented in previous studies. One novel phosphorylation site, S87, was discovered.

**Conclusions and Relevance:** Optimization of phosphoenrichment of digested frontal cortex brain samples using novel technology, such as the Agilent AssayMap Bravo platform, offers an important methodological advancement for future studies seeking to investigate phosphorylated aSyn biomarkers in PD. The discovery of pS87 in erythrocytes warrants further evaluation in future research as a potential biomarker for early PD diagnosis, which could improve health outcomes in affected patients.

Identification of a Novel Phosphorylation Site on Alpha-Synuclein Within Erythrocyte Ghost  
Membranes

By

Joshua Chiok

Blaine Roberts, PhD.

Advisor

A thesis submitted to the Faculty of Emory College of Arts and Sciences  
of Emory University in partial fulfillment  
of the requirements of the degree of  
Bachelor of Sciences with Honors

Neuroscience and Behavioral Biology

April 10, 2024

## Acknowledgments

I would like to thank Dr. Blaine Roberts for giving me the opportunity to conduct research in his laboratory at Emory University. His guidance throughout this process was instrumental to my development as a student. I would like to thank Dr. Shaima Nazaar for her support and oversight throughout this project. I would like to thank Anne Roberts for her introduction to the Robert's lab and her guidance throughout. I would like to thank Lester Manly for taking his time to provide mentorship and advice during the development of the thesis. I would like to thank Ankit Jain for his insight in the data analysis software. I would like to thank the entirety of the Robert's Lab for their help in my development as a researcher. I would like to thank my committee members, Dr. Benítez and Dr. Weinschenk, for their excellent instruction, dedicated time, and valuable input into my thesis. I would like to thank my family and friends for their continual support, especially my father Joseph Chiok, my mother Martha Chiok, and my brothers, Ivan and Benjamin Chiok.

## Table of Contents

Abstract.....	1
Introduction.....	3
Figure 1. Previously described alpha-synuclein phosphorylation sites in the literature.....	7
Methods.....	11
Figure 2. Schematic Workflow of TiO <sub>2</sub> Phosphoenrichment.....	15
Results.....	16
Figure 3. Glycolic Acid Optimization of Bravo Fe-NTA Binding Buffer.....	17
Figure 4. Acetonitrile Optimization of Bravo Fe-NTA Elution Buffer.....	18
Figure 5. Fe-NTA vs TiO <sub>2</sub> Phosphopeptide Comparison.....	20
Figure 6. Erythrocyte Ghost Membrane Sample Load Optimization for Phosphoenrichment.....	21
Figure 7. Y125, S87, and S129 Alpha-Synuclein Phosphorylation Sites in Erythrocyte Ghost Membranes .....	23
Discussion.....	25
Future Directions.....	33
References.....	35

## Abstract

**Background:** Parkinson's disease (PD) is the second most prevalent neurodegenerative disorder and is on the rise within the aging population of the United States. PD is typically detected during its advanced stages, when significant neuron degeneration has occurred. The challenge of diagnosing PD early is of the utmost importance, with significant implications for improving the overall quality of life of individuals living with the disease. A potential solution to achieving early PD diagnosis lies in the development of minimally invasive diagnostic biomarkers such as the detection of phosphorylated alpha-synuclein in RBCs utilizing mass spectrometry. The goal of this study is to discover novel phosphorylation sites in erythrocyte ghost membranes that can later be evaluated as potential biomarkers for diagnosing PD.

**Methods:** A pool of RBCs were obtained from The Australian Imaging, Biomarker & Lifestyle Flagship Study of Ageing (AIBL). Erythrocyte ghost membranes were extracted from the AIBL pool of RBCs and then underwent phosphoenrichment via immobilized metal affinity chromatography using the Agilent AssayMap Bravo platform. After phosphoenrichment, samples were placed in a Bruker TimsTof Flex coupled to either an Evosep nano HPLC or Bruker nanoelute2 HPLC. Data was acquired using a default data dependent acquisition (DDA) method on MS. Data was analyzed using Skyline and FragPipe software.

**Results:** 0.5% glycolic acid in the binding buffer of Fe-NTA IMAC phosphoenrichment was optimal. 10% acetonitrile in the elution buffer of Fe-NTA IMAC phosphoenrichment was optimal. Fe-NTA IMAC had a greater percentage of unique phosphopeptides and contained our target protein alpha-synuclein in comparison to our TiO<sub>2</sub> OMAC phosphoenriched samples that

did not contain alpha-synuclein. 100 µg of erythrocyte ghost membranes was the optimal sample load for MS analysis. Alpha-synuclein was found to be phosphorylated at Y125 and S129 as documented in previous studies. One novel phosphorylation site, S87, was discovered.

***Conclusions and Relevance:*** Optimization of phosphoenrichment of digested frontal cortex brain samples using novel technology, such as the Agilent AssayMap Bravo platform, offers an important methodological advancement for future studies seeking to investigate phosphorylated aSyn biomarkers in PD. The discovery of pS87 in erythrocytes warrants further evaluation in future research as a potential biomarker for early PD diagnosis, which could improve health outcomes in affected patients.

## Introduction

Parkinson's disease (PD) is the second most prevalent neurodegenerative disorder and is on the rise within the aging population of the United States (Connolly and Lang, 2014). PD typically results from a loss of dopaminergic neurons and the aggregation of neuronal Lewy Bodies (LBs), which causes decreased amounts of dopamine. Dopamine is a neurotransmitter that is responsible for several important functions including coordination of movement, reward, pleasure, concentration, and emotion (Schultz, 2007). Reduced dopamine levels in individuals with PD commonly results in diminished motor coordination, altered behavior consistent with depression, and cognitive impairments, particularly dementia. While there are currently treatments that address the dopamine deficiency in patients with PD, such as Levodopa, these therapies have demonstrated the ability to provide symptomatic relief but have not shown the capacity to halt the progression of PD.

In addition to the limited availability of treatments for preventing the progression of PD, the disease is typically detected during its advanced stages, when significant neuron degeneration has occurred. This results in a diminished quality of life where treatment options are more limited and have reduced effectiveness. The challenge of diagnosing PD early is of the utmost importance, with significant implications for improving the overall well-being of individuals living with the disease. A potential solution to achieving early PD diagnosis lies in the development of diagnostic biomarkers, particularly those associated with the formation of Lewy Bodies, which are a primary contributor to PD development. Lewy bodies are abnormal intraneuronal cytoplasmic clumps of protein that are known to accumulate and disrupt parts of the brain responsible for memory and muscle movement such as the basal ganglia and hippocampus (Haider et al., 2023; Oliveira Manzanza et al., 2021). While Lewy body formation

is not fully understood, research suggests that the aggregation of a protein called alpha-synuclein could play a pivotal role.

Alpha-synuclein (aSyn) is a peripheral membrane protein believed to play a role in synaptic transmission. This belief is supported by findings demonstrating that overexpression of aSyn inhibits neurotransmitter release (Nemani et al., 2010). A study first discovered aSyn when they used monoclonal antibody 11.57 to recognize PHF-tau and fetal tau, but the antibody labeled an additional two 19 kDa protein bands with lengths of 140 and 134 amino acids; the 140 amino acid protein was termed  $\alpha$ -synuclein (Jakes et al., 1994). It was later found that aSyn was a primary component of Lewy bodies in PD after a study stained Lewy bodies with antibodies specific to aSyn, which then revealed their immunopositivity (Grazia Spillantini et al., 1997).

The expression of aSyn typically occurs due to an imbalance in dynamic equilibrium, where aggregated aSyn increases while soluble aSyn decreases (Manzanza et al., 2021). This imbalance perpetuates the formation of beta-sheet assemblies that precede Lewy body formations (Estaun-Panzano et al., 2022). This loss of equilibrium is thought to be influenced by post-translational modifications (PTMs) that alter aSyn's structure and solubility. Of particular significance is the aSyn PTM of phosphorylation. The first study investigating phosphorylated aSyn found that aSyn phosphorylation was regulated predominantly at two major phosphorylation sites: serine 129 (S129) and serine 87 (S87) (Okochi et al., 2000). Since the discovery of phosphorylation sites on aSyn, studies have validated the importance phosphorylation plays in the aggregation of aSyn, such as a study that showed that aSyn external fibrils lead to the accumulation of cellular aggregates containing phosphorylated aSyn (Kawahata et al., 2022). The accumulation of phosphorylated S129 (pS129) in aSyn has been documented in several animal models and patient studies on PD, which highlights the importance

of this PTM and potential implications for diagnostic capabilities (Chen and Feany, 2005; Yamada et al., 2005; Samuel et al., 2016).

Frequently stated in the literature is a statistic that indicates that approximately 90% of aSyn found in Lewy bodies is phosphorylated at S129 in PD patients, whereas only around 4% of aSyn exhibits this modification in healthy individuals (Fujiwara et al., 2002; Xu et al., 2015; Manzanza et al., 2021). However, these percentages are questionable since they were attained by extrapolating the proportion of phosphorylated aSyn relative to the total aSyn in urea-soluble fractions of dementia with Lewy body (DLB) brains, which was done by estimating the intensities of bands observed in DLB samples (Fujiwara et al., 2002). Band intensities were measured using densitometry via an NIH-image program. Using intensities from SDS-PAGE bands relies on various factors, including background correction, reproducible quantification, and antibody selection. However, this method lacks a standard curve, rendering the results semiquantitative (Kroon et al., 2022). Along with the questionable validity of quantitation from the intensities of bands, the paper assumes that the identity of the intensity of the bands is from phosphorylated aSyn that is entirely from pS129, when in reality the antibody they used, anti-pS129, is a polyclonal antibody that targets multiple epitopes and has a broader range of binding sites than just pS129. This assumption is therefore unfounded and contributes to the misleading 90% statistic. Additionally, the study assumes that their standard aSyn is fully phosphorylated at S129 by casein kinase 2; however, there is no evidence to show the purity of their standard and thus the control that they are comparing their samples to is questionable. This frequently referenced statistic and its glaring oversights highlight the need for better quantification approaches to measuring aSyn. While this statistic may be inflated, several studies have confirmed the established tendency for elevated phosphorylated aSyn levels in PD (Tu et

al., 2021; Arawake et al., 2017; Chen and Feany, 2005). Therefore, aSyn phosphorylation sites could serve as a promising biomarker, holding potential for early-stage PD diagnosis, but requires further work to validate the accuracy and precision of phosphorylation sites in aSyn. Further investigation using mass spectrometry (MS) techniques could help validate or invalidate these study's findings.

The biospecimen type of a biomarker is important when considering PD diagnosis. Biomarkers ideally have high specificity, sensitivity, accuracy, reproducibility, stability, biological relevance, cost effectiveness, and should be minimally invasive (Califf, 2018). Although phosphorylation of aSyn in the brain and cerebrospinal fluid (CSF) have undergone testing (Figure 1B), obtaining brain and CSF samples involves invasive procedures that are not feasible in many clinical settings. This has prompted research into alternative biospecimen types, such as blood.

Blood is readily accessible, minimally invasive, and contains a high abundance of aSyn (Klatt et al., 2020). Only a limited number of studies have investigated the phosphorylation sites of aSyn in erythrocytes due to the significant interference from highly abundant proteins, particularly hemoglobin, which complicates the discovery of potential proteomic biomarkers (Klatt et al., 2020). A solution to this issue are erythrocyte ghost membranes since they have their inner contents, such as hemoglobin, removed and have only their membrane and structural components left behind (Mohandas and Gallagher, 2008). With the use of erythrocyte ghost membranes, there is effective hemoglobin removal and wide-ranging recovery of RBC membrane proteins of low and high abundance (Fye et al., 2018). Hence, by focusing on RBC ghost membranes, this study enables more precise analysis of aSyn, given its nature as a membrane protein. Additionally, the depletion of hemoglobin and the excellent recovery of a

diverse set of proteins enhances the sample's preparation for MS analysis. Therefore, red blood cells (RBCs) hold significant promise as a potential biomarker medium for PD despite the interference of hemoglobin. Of the few studies that have investigated RBC aSyn phosphorylation sites, only two phosphorylation sites have been described in the literature: tyrosine 125 (Y125) and S129 (Figure 1A). These investigations have identified elevated levels of phosphorylated aSyn in individuals with PD compared to healthy controls, as determined by immunoassays (Vicente Miranda et al., 2017; Foulds et al., 2011; Cariulo et al., 2019). These investigations consistently underscore the necessity for more sensitive assays to deepen our understanding and measurement of aSyn phosphorylation in RBCs, a challenge that can be met with MS.

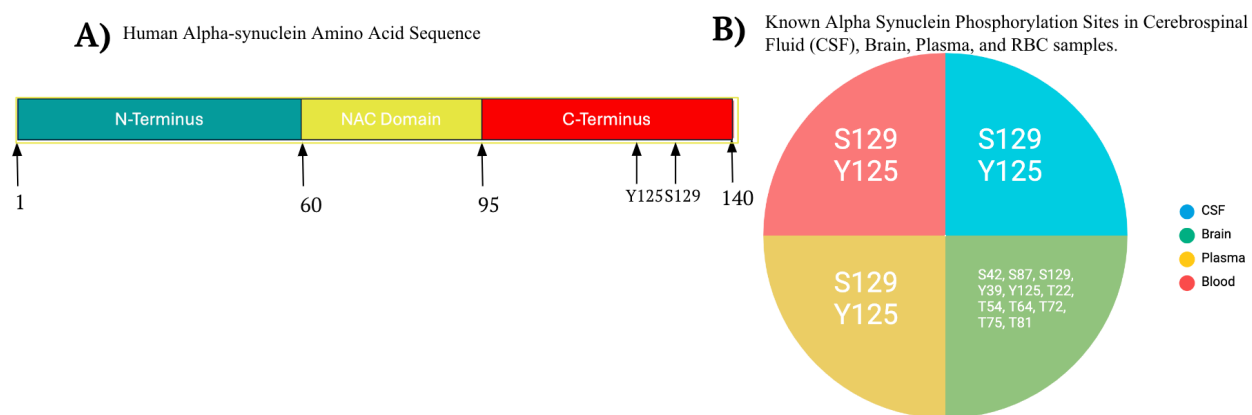


**Figure 1. Previously described alpha-synuclein phosphorylation sites in the literature.**

(A) The amino acid sequence of human alpha-synuclein is 140 amino acids long. The two phosphorylation sites that are found in RBCs are shown by arrows at the C-terminus, which are serine 129 (S129) and tyrosine 125 (Y125). (B) Summarization of known alpha-synuclein phosphorylation sites in different biological mediums, including cerebrospinal fluid (CSF), brain, plasma, and RBC samples. There are 11 documented aSyn phosphorylation sites across different brain types including mice and humans, while there are only 2 documented phosphorylation sites

in CSF, RBC, and plasma. (Vicente Miranda et al., 2017; Li et al., 2021; Tian et al., 2019; Lin et al., 2019; Foulds et al., 2013; Cariulo et al., 2019; Wang et al., 2012; Kalia, 2018; Constantinidines et al., 2021; El Turk et al., 2018; Mahul-Mellier et al., 2014; Xu et al., 2015; Zhang et al., 2023).

Mass spectrometers are instruments used to analyze, identify, and quantify the chemical composition of substances by separating ions based on their mass-to-charge ratio ( $m/z$ ). MS changes molecules into ions by using an ion source, which is then sorted based on their  $m/z$  by a mass analyzer and measured and displayed as chromatograms and mass spectra as detected by a mass analyzer (Garg and Zubair, 2023). Previous studies using immunoassays are surpassed by the unparalleled sensitivity, specificity, low detection limits, and minimal sample requirements offered by MS (Tajik et al., 2022). While immunoassays are widely available and more economically friendly in comparison to MS, they have limited specificity due to potential cross-reactivity with similar molecules, limited detection of one analyte at a time whereas MS can have simultaneous detection of multiple analytes, and immunoassays rely on specific antibodies that have a narrower quantification range than MS (Sturgeon and Viljoen, 2011; Ohlsson et al., 2013). Thus, MS is a novel and improved assay in comparison to previous studies investigating erythrocyte phosphorylated aSyn, as immunoassays were previously the exclusive method utilized.

Immobilized metal affinity chromatography (IMAC) is a standard method for phosphopeptide enrichment of samples. This technique purifies proteins by selectively binding them to metal ions fixed in place to resin based on their degree of attraction. This attraction is caused by the negatively charged phosphate groups towards positively charged metal ions, such

as  $\text{Fe}^{3+}$  (Thingholm and Larsen, 2016). IMAC is conventionally performed manually through batch incubation with beads containing the desired metal ions or via a micro-column that is packed with beads. However, a novel and more efficient approach involves the utilization of a robotic automated protein preparation platform, the Agilent AssayMAP Bravo platform. This platform uses precise liquid control and specialized Fe(III)-Nitriloacetate (Fe-NTA) cartridges that are shown to reduce sample preparation variability and provide reproducible enrichment of phosphopeptides (Russell and Murphy, 2015). With the application of the AssayMAP Bravo platform, we are able to ensure that phosphoenriched erythrocyte samples have decreased variation and high reproducibility for up to 96 samples, which is on a significantly larger scale than manual methods.

Metal oxide affinity chromatography (MOAC) is another common method for phosphopeptide enrichment of samples. IMAC has metal ions fixed onto solid support to create an affinity matrix, which is necessary for the regulated presentation of metal ions. However, MOAC uses the metal oxides within itself as a matrix so that resin is not necessary (Fila and Honys, 2011).  $\text{TiO}_2$  is the most used phosphopeptide enrichment MOAC strategy after several experiments proved it had a high and constant yield of phosphopeptides (Fila and Honys, 2011).  $\text{TiO}_2$  has also been shown to have identified 50% different phosphopeptides than IMAC Fe-NTA, which could signify its importance in conjunction with Fe-NTA to cover the entire phosphoproteome (ThermoFisher Scientific, 2024). Therefore, we used both MOAC and IMAC in this study because of their differences in selectivity and specificity towards phosphopeptides.

This study focuses on optimizing phosphoenrichment of erythrocyte ghost membranes and analyzing these samples, particularly targeting the phosphorylation sites of aSyn proteins. We will employ MS with a DDA approach alongside proteomic analysis software to explore

potential novel aSyn phosphorylation sites within erythrocyte ghost membranes while also validating previously documented ones. By utilizing this assay, we anticipate achieving heightened sensitivity and precision compared to previous immunoassays used for assessing aSyn phosphorylation in blood samples.

## Methods

### **Human blood collection:**

RBCs were obtained from The Australian Imaging, Biomarker & Lifestyle Flagship Study of Ageing (AIBL) and were isolated as previously described (Klatt et al., 2020; Roberts et al., 2016; Ellis et al., 2009). AIBL is a longitudinal study of ca. 1000 individuals aged over 60 years of age, designed to develop a better understanding of both imaging and blood-based biomarkers for Alzheimer's disease and PD. Experiments were conducted under University of Melbourne human ethics committee approval ID1136882.

### **Erythrocyte Ghost Membrane Digest:**

A protocol was utilized in order to separate erythrocyte's ghost membrane from RBCs. First, obtain 40 $\mu$ L of undiluted (neat) RBCs in 1.77 mL Eppendorf tubes. To the RBCs, 160  $\mu$ L of 5 mM Na<sub>2</sub>HPO<sub>4</sub>, 0.35 mM ethylenediaminetetraacetic acid (EDTA) with protease inhibitor at pH 8 was then added. A ratio 1:5 of RBC volume to buffer volume must be maintained if changes are made. After vortexing, the solution was centrifuged at 8000 x g for five minutes. A pellet at the bottom of a tube was formed after centrifugation. The supernatant was carefully removed so as to not disturb the pellet. Once the supernatant is removed, the pellet was washed with 5 mM Na<sub>2</sub>HPO<sub>4</sub>, 0.35 mM EDTA buffer without protease inhibitor and centrifuge at 8000 x g for two minutes. The supernatant was then removed and the pellet was washed up six to eight times. After washing, the pellet became clear and appeared white or "ghost" like. Ghost membranes were then reduced, alkylated, and denatured (RAD) at 95 °C for 10 minutes with a 1x final concentration of 50  $\mu$ L of RAD buffer consisting of 1% deoxycholate for denaturation, 40 mM of 2-chloroacetamide (CAA) for alkylation, and 10 mM tris(2-carboxyethyl)phosphine (TCEP) for reduction. The samples were allowed to reach room temperature before a brief

centrifugation step. Trypsin (#90305) was added then added at a ratio of 1:20 (enzyme amount to sample protein amount) and placed into an incubator at 37 °C overnight for digestion. This step is crucial as it fragments large proteins into smaller peptides. The following day, the samples were then acidified with formic acid (FA) to a final concentration of 5%. This step was performed to quench the reaction and to remove the deoxycholate denaturant from the sample. The sample was then mixed at room temperature on an oscillator for 30 minutes and then centrifuged at 18,000 x g for 20 minutes. Solid phase extraction (SPE) clean-up was then performed to remove non-MS compatible compounds from the samples. For SPE clean-up, Waters, Oasis® PRiME HLB 10 mg plate (#186008053) were utilized following manufacturer's instructions with modification of eluting the samples of the plate using 1.5x column volumes of 80% ACN 0.1% TFA, and 0.5% GA for subsequent phosphoenrichment. After performing SPE clean-up, the samples are dried down in a Labconco acid-resistant CentriVap® concentrator vacuum and centrifuged at 70 °C until the tubes are dry. The samples were then resuspended with 30 µL of LC-MS grade water with 0.1% FA and allowed to resuspend on an oscillator for 30 minutes. The peptide concentration is estimated using an Eppendorf BioSpectrometer and a Eppendorf µCuvette® G1.0 at an absorbance of 280 nm, providing insight into the amount of sample that can be loaded onto the MS.

### **TiO<sub>2</sub> Phosphopeptide Enrichment:**

For TiO<sub>2</sub>, a ThermoFisher Scientific TiO<sub>2</sub> MOAC kit (ThermoFisher Scientific: A32993) was utilized following the manufacturer's provided protocol, starting with the desalting of 0.5 - 1.0 mg of peptide sample. Peptides were completely resuspended in the binding buffer and the pH was verified to be below 3. The sample was then applied to a TiO<sub>2</sub> spin tip and centrifuged to

capture phosphopeptides. After several wash steps, phosphopeptides were eluted with an elution buffer and dried in a vacuum centrifuge. The dried eluate was then resuspended in 0.1% formic acid and centrifuged before aspirating for MS analysis.

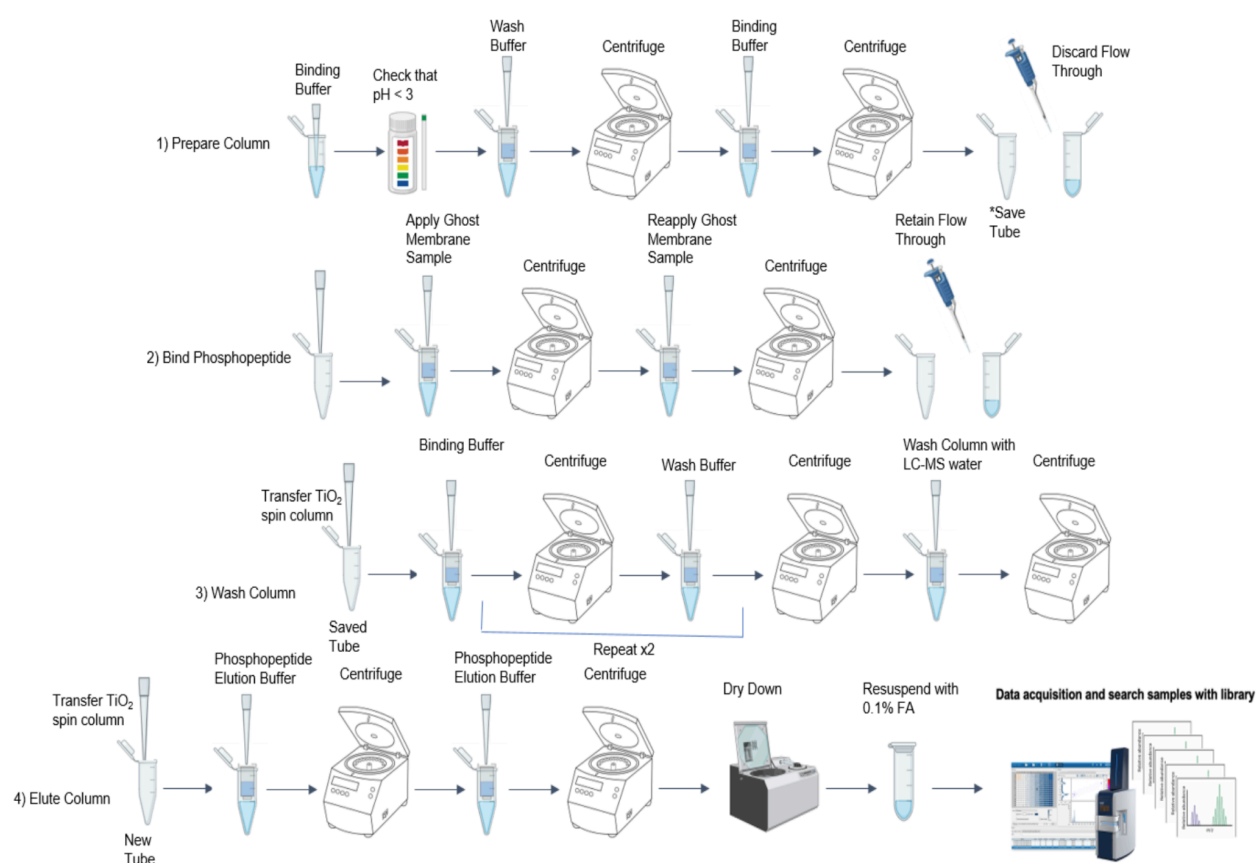


**Figure 2. Schematic Workflow of  $\text{TiO}_2$  Phosphoenrichment:** Phosphorylation enrichment of aSyn from erythrocyte ghost membranes. This schematic shows the steps taken to prepare the  $\text{TiO}_2$  column, bind the phosphopeptide, wash the column, elute, prepare sample for MS, and subsequent analysis.

**Agilent AssayMAP Bravo Fe (III)-NTA Phosphoenrichment:**

Phosphopeptide enrichment protocol using Fe (III)-NTA cartridges was followed per application notes (Russell and Murphy, 2016). A first round of optimization for this phosphoenrichment protocol focused on exploring different concentrations of glycolic acid (GA) in the initial binding buffer, which enhanced the phosphoenrichment binding. After testing varying concentrations, 0.5% GA produced the best total quantity of phosphoenriched peptides. After optimizing the addition of GA, the next objective was to verify the presence of all the phosphopeptides intended to retain in the elution, primarily aSyn peptides. This was accomplished by experimenting with various acetonitrile (ACN) percentages in the elution buffer. The following concentrations of ACN, 0%, 10%, 30% and 50%, were tested to see if there was any benefit in the number of phosphopeptides measured. In short, the samples were placed on the Bravo in their SPE binding buffer, 80% ACN, 0.1% trifluoroacetic acid (TFA), 0.5% GA, and tips were primed with 99.9% ACN, 0.1% TFA. They were equilibrated with 80% ACN, 0.1% TFA before loading the sample. Tips underwent a wash step with the 80% ACN, 0.1% TFA before being eluted with 1% NH<sub>4</sub>OH, 10% ACN.

**Data Acquisition:**

Data was acquired using a Bruker TimsTof Flex coupled with a Bruker nanoElute2 nanoflow high performance liquid chromatography instrument (nanoHPLC). Data was acquired using a default data dependent acquisition (DDA) method on MS. Data collected on the nanoElute2 nanoHPLC used a 15 cm IonOpticks column with a 44 min gradient using a mobile phase A consisting of 0.1% FA with water and a mobile phase B consistent of 0.1% FA in ACN. Gradients were starting at 5% mobile phase B to 70% mobile phase B over the course of the 44

minute gradient. Software such as FragPipe and Skyline were utilized to identify the phosphopeptides within each sample following MS analysis. MBR-LFQ phospho-workflow was applied.

## Results

### **Optimizing Phosphoenrichment Binding Buffer with Glycolic Acid:**

For this study, the first goal was to optimize the phosphoenrichment method for samples using the Bravo platform. To do this, front cortex was utilized due to sample availability since erythrocyte ghost membranes needed to be generated manually. 250  $\mu\text{g}$  of frontal cortex brain samples were digested with trypsin, which are proteolytic enzymes that cleave peptide bonds at lysine and arginine residues to generate peptides. The brain digested samples then underwent varying amounts of GA in the binding buffer ranging from 0% to 2%. GA enhances specificity when added to the binding buffer of the Fe-NTA kit, so it is of utmost importance to optimize this amount. As can be seen in figure 3A, 0.5% GA had the greatest coverage of phosphopeptides (serine, threonine, and tyrosine; STY) and the highest percent enrichment at 73.2%. While the 1% GA treatment resulted in the same percentage of enrichment, it yielded fewer phosphopeptides than 0.5% GA, as can be seen in figure 3B. The aim was to maximize the presence of phosphopeptides in the sample to enhance the likelihood of detecting phosphorylated aSyn.

A) Glycolic Acid %	0	0.2	0.5	1	2
Total peptides	27237	28073	24399	23939	27770
STY peptides	15313	16334	17864	17524	17659
% enrichment	56.2	58.2	73.2	73.2	63.6

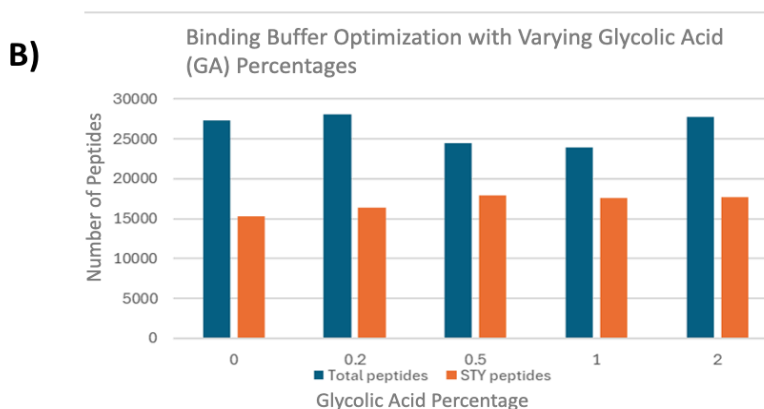


**Figure 3. Glycolic Acid Optimization of Bravo Fe-NTA Binding Buffer:** The 80% acetonitrile (ACN), 5% trifluoroacetic acid (TFA), 0.5% GA binding buffer was identified as optimal because it exhibited the highest percentage of enrichment and yielded the greatest quantity of STY peptides. (A) Comparison of the total peptides, phosphorylated STY (serine, threonine, tyrosine) peptides, and percent enrichment of different glycolic acid percentages in binding buffer. (B) The graph presents a comparison between the total number of peptides in each glycolic acid concentration and the number of STY peptides.

### Optimizing Phosphoenrichment Elution Buffer with Acetonitrile:

After the enhancement of the binding buffer, the elution buffer was optimized with the addition of acetonitrile (ACN). The decision to add ACN was made because it is an organic solvent that assists in the elution of hydrophobic proteins, such as aSyn. 250  $\mu$ g of frontal cortex brain samples were digested with trypsin and lysC and then underwent varying amounts of ACN in the elution buffer ranging from 0% to 50%. As depicted in Figure 4A, both 10% ACN and

50% ACN showed the highest phosphopeptide enrichment at 89%, with comparable amounts of total peptides and STY peptides. However, 50% ACN displayed slightly higher quantities as visualized in figure 4b. Although 50% ACN had slightly higher quantities, 10% ACN was chosen as the addition to the elution buffer since it is allowed for immediate injection into the high-performance liquid chromatography (HPLC), which goes from a low to high concentration of organic solvent.

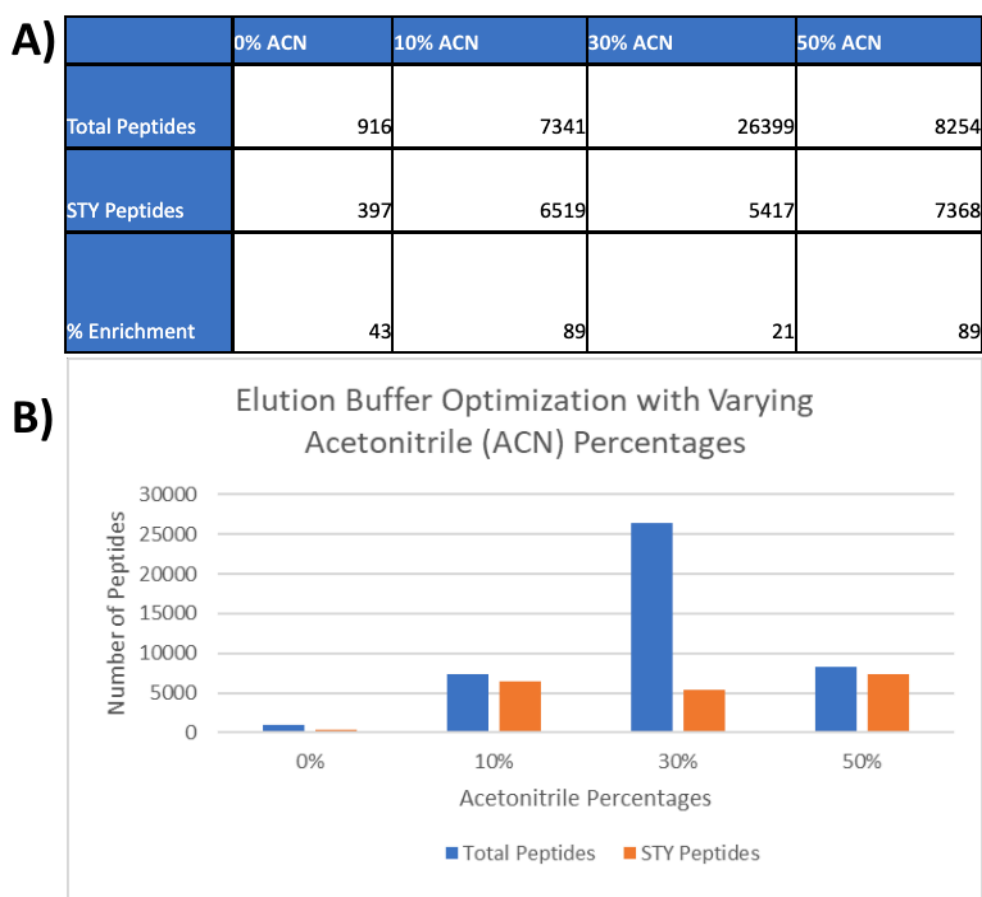


**Figure 4. Acetonitrile Optimization of Bravo Fe-NTA Elution Buffer:** The 10% ACN, 1%  $\text{NH}_4\text{OH}$  elution buffer was identified as optimal because it exhibited the highest percentage of phosphoenrichment and yielded a large quantity of STY peptides. (A) Comparison of the total peptides, phosphorylated STY peptides, and percent enrichment of different ACN percentages in

elution buffer. (B) The graph presents a comparison between the total number of peptides in each ACN concentration and the number of STY peptides.

### **Fe-NTA vs TiO<sub>2</sub> Phosphopeptide Enrichment Comparison:**

This study aimed to employ and compare both Fe-NTA and TiO<sub>2</sub> techniques to encompass a greater portion of the RBCs' phosphoproteome, thereby increasing the likelihood of detecting phosphorylated aSyn. Figure 5A demonstrates that all brain digested samples subjected to TiO<sub>2</sub> phosphoenrichment exhibit a comparable amount of STY peptides. Notably, the 1 mg TiO<sub>2</sub> phosphoenriched brain sample exhibited reduced non-specific binding, resulting in a higher percentage of enrichment compared to the TiO<sub>2</sub> phosphoenriched 500 µg brain samples. On the contrary, the Fe-NTA phosphoenriched brain digest samples consistently exhibit higher specific binding, as indicated by their percent enrichment displayed above the bar graphs (Figure 5B). However, they exhibit a lower total number of STY peptides overall, with 500 µg showing the highest number (4,486) of STY peptides and being the preferred sample load (Figure 5B). When comparing both the TiO<sub>2</sub> and Fe-NTA phosphoenriched 500 µg digested brain samples, it is shown that Fe-NTA has more unique phosphopeptides than TiO<sub>2</sub> (48% > 18.7%, respectively) and that they shared 33.3% of the same phosphopeptides (Figure 5C). Additionally, the OMAC TiO<sub>2</sub> phosphoenrichment technique did not have any aSyn present within the sample. Therefore, IMAC Fe-NTA is the preferred phosphoenrichment technique since it contains our protein of interest (aSyn), covers the most unique phosphopeptides, and has the highest percent enrichment.

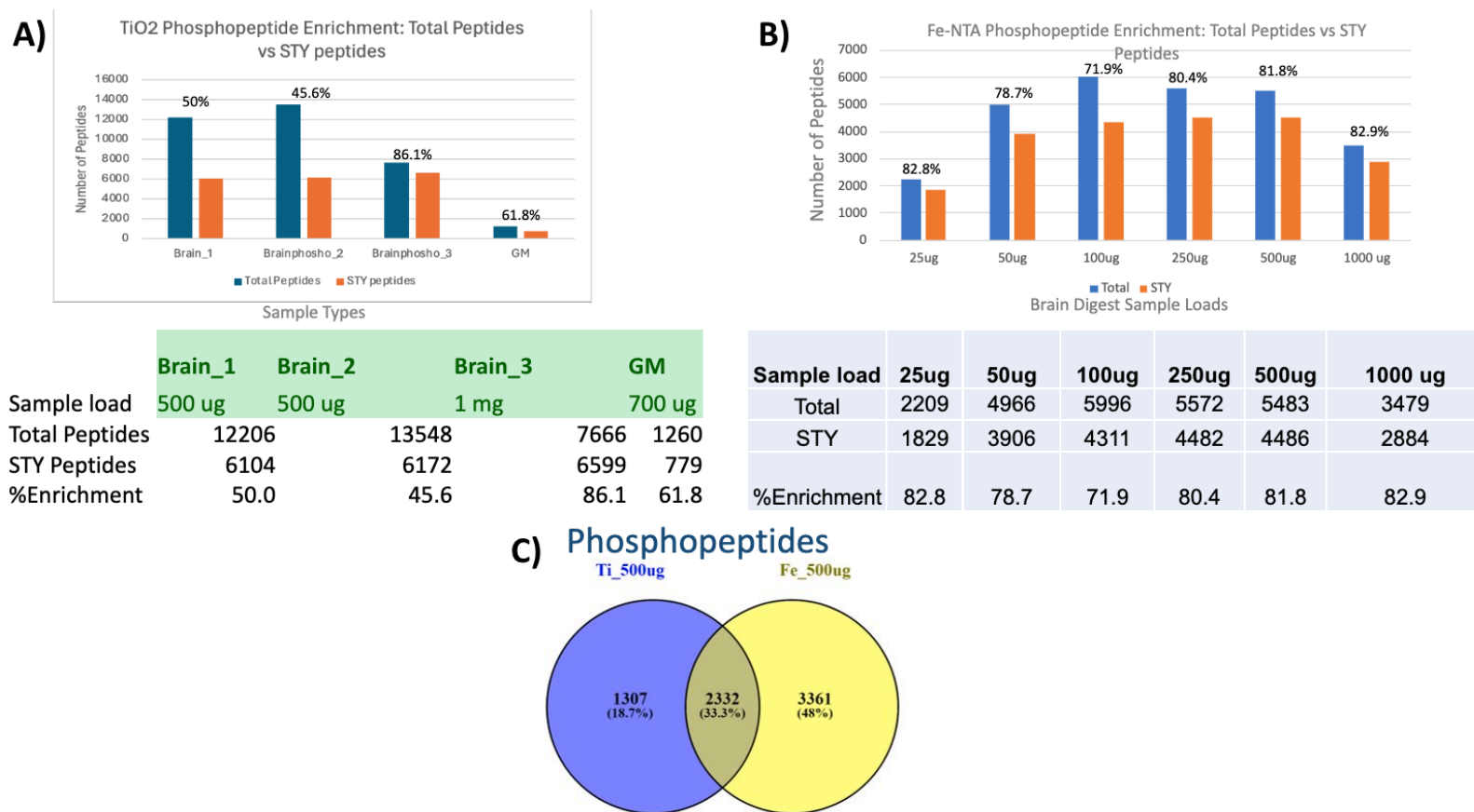


**Figure 5. Fe-NTA vs TiO<sub>2</sub> Phosphopeptide Comparison:** IMAC Fe-NTA phosphoenrichment has the highest quantity of unique phosphopeptides and the best specific-binding in comparison to OMAC TiO<sub>2</sub>. (A) Comparison of the total peptides, phosphorylated STY peptides, and percent enrichment of different sample loads and sample types subjected to TiO<sub>2</sub> phosphoenrichment. (B) Comparison of the total peptides, phosphorylated STY peptides, and percent enrichment of different sample loads of frontal cortex brain digestion subjected to Fe-NTA phosphoenrichment. (C) Venn diagram showing the percentage of unique phosphopeptides between TiO<sub>2</sub> vs Fe-NTA phosphoenriched 500 µg frontal cortex brain digested samples.

### Optimizing Erythrocyte Ghost Membrane Sample Load:

After fine-tuning the binding and elution buffers, the sample loading for ghost membranes needed to be optimized for phosphoenrichment. Figure 6A demonstrates the different ghost membrane ( $\mu\text{g}$ ) sample loads (6, 12, 25, 50, 100  $\mu\text{g}$ ) and their number of total peptides, STY peptides, and percent enrichment. The 100  $\mu\text{g}$  sample load had the highest quantity of phosphopeptides (894), with significantly more total peptides (948) compared to the other sample loads (Figure 6B). It was concluded that the 100  $\mu\text{g}$  ghost membrane was the optimal sample load moving forward not only because of the great quantity of phosphopeptides, but also because within the 100  $\mu\text{g}$  sample there was a newly observed aSyn phosphorylation site, S87 (Figure 7C, D, E).

A) Sample load( $\mu\text{g}$ )	100	50	25	12	6
Total	948	623	255	160	172
STY	894	604	243	137	111
%Enrichment	94.3	97.0	95.3	85.6	64.5

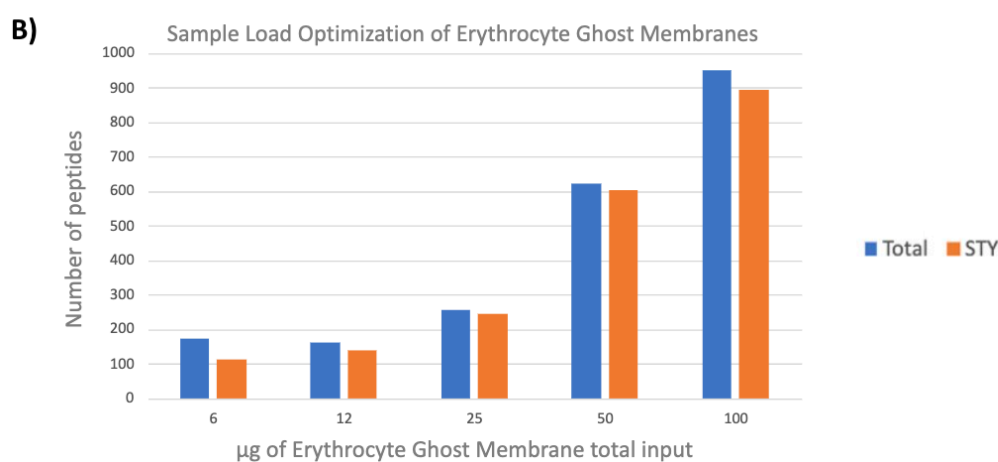


### Figure 6. Erythrocyte Ghost Membrane Sample Load Optimization for

**Phosphoenrichment:** The 100  $\mu\text{g}$  sample load was identified as optimal because it exhibited the greatest quantity of STY peptides along with a 94.3% phosphoenrichment. (A) Comparison of

the total peptides, phosphorylated STY peptides, and percent enrichment of different erythrocyte ghost membrane sample loads ( $\mu\text{g}$ ). (B) The graph presents a comparison between the total number of peptides in each sample load and the number of STY peptides.

### **Alpha-Synuclein Phosphorylation Sites in Erythrocyte Ghost Membranes:**

After phosphoenrichment and MS analysis, raw data files were processed using both Skyline software and the FragPipe computational platform. We discovered three phosphorylation sites of aSyn on the erythrocyte ghost membrane: Y125, S87, and S129, which are highlighted in the amino acid sequence of aSyn and marked with stars (Figure 7A). The specific peptide fragment sequences identified by FragPipe, along with their phosphorylation sites, are listed in Figure 7B. Afterwards, we wanted to further confirm the presence of these phosphorylation sites by generating extraction ion chromatograms targeting the newly discovered aSyn phosphopeptides pY125, pS87, and pS129. The representative chromatographic peaks displayed in Figure 7C are indicative of the presence of pY125, pS87, and pS129, respectively. The presence of peaks on the extracted chromatograms indicate the identity of the peptides pY125, pS87, and pS129 and the area under the curve of the respective peaks show relative amounts of peptide. This is further confirmed by an ion mobiligram that shows that the peak of the chromatogram is one population of ions (Figure 7D). The ion density as a singular population of ions in the ion mobility window enhances the reliability of the data. Figure 7E shows the fragmentation spectra for pY125, pS87, and pS129. The fragmented sequence is shown above with the phosphorylation site highlighted. The b23 ion is diagnostic for the presence of pY125 in the first fragmentation spectra. The following ions are diagnostic for the presence of pS87: b15, b13, b9, b8, b7, y10, y11, y12, y13, y14, y15. The y13 ion is diagnostic for pS129.



**B)**

Peptide	Sequence
pY125	NEEGAPQEGI LEDMPVDPDN EAYEMPSEEG YQDYEPE(A)
pS87	TVEGAG[S]IAAATGFV(K)
pS129	NEEGAPQEGI LEDMPVDPDN EAYEMP[S]EEG YQDYEPE(A)

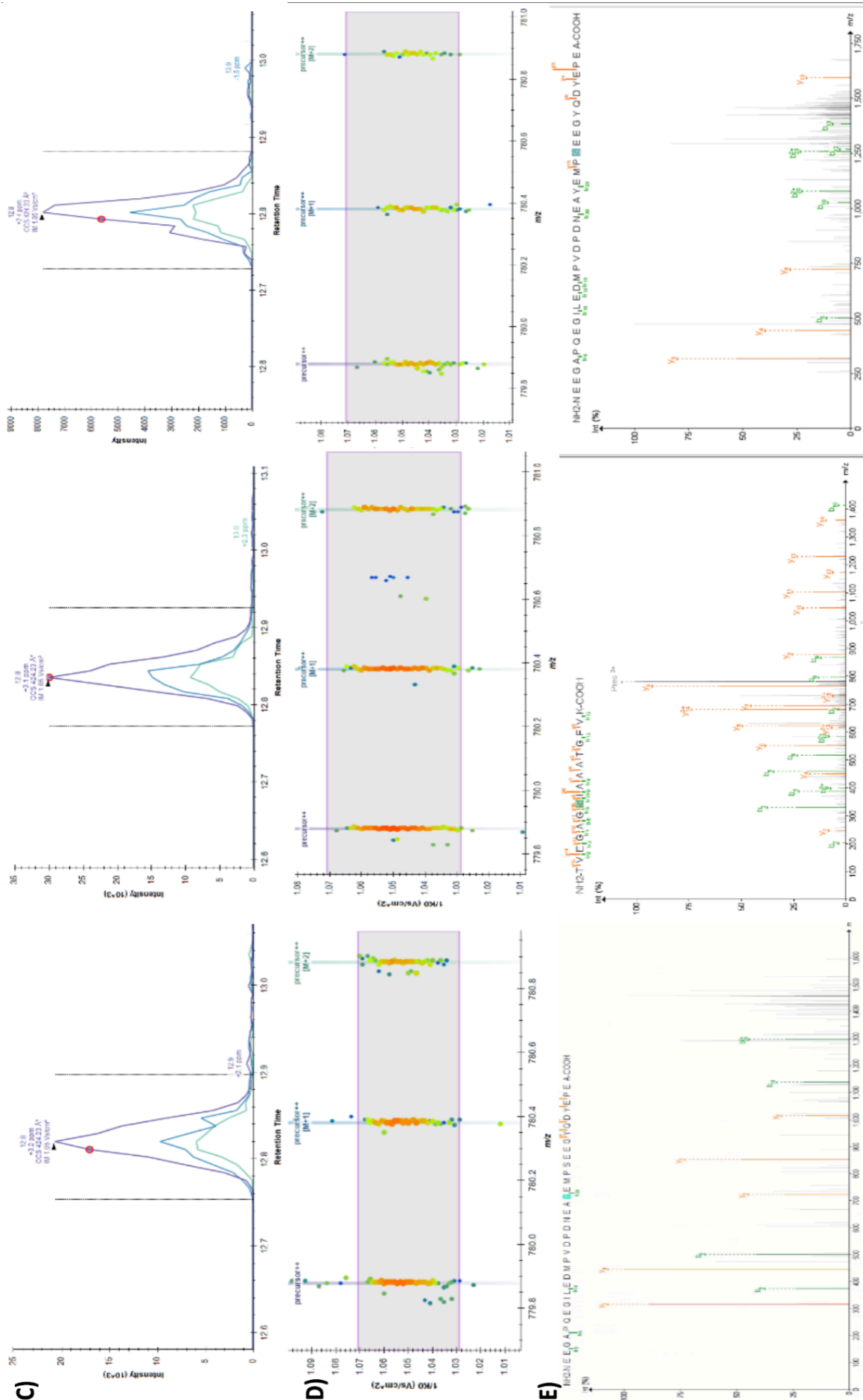


**Figure 7. Y125, S87, and S129 Alpha-Synuclein Phosphorylation Sites in Erythrocyte Ghost**

**Membranes:** Previously cited phosphorylation sites of aSyn in RBCs, Y125 and S129, were validated in erythrocyte ghost membranes. Additionally, a new phosphorylation site, S87, was discovered in this study. (A) The study's documented phosphorylation sites on aSyn's amino acid sequence, shown by red highlight and red stars for the phosphorylated serine amino acids and orange highlight and an orange star for the phosphorylated tyrosine residue. (B) Table listing the peptide fragment sequences containing our identified phosphorylation sites (highlighted red if serine and orange if tyrosine). (C) Representative chromatographic peaks of pY125, pS87, and pS129, respectively. (D) Ion mobiligram of each corresponding peak that further confirms the presence of the aSyn phosphorylation sites. (E) Fragmentation spectra for pY125, pS87, and pS129 respectively. Each spectra has b and y ions that are diagnostic for the presence of the aforementioned phosphorylation sites.

## Discussion

The optimization of phosphopeptides in digested frontal cortex brain samples using novel technology, such as the Agilent AssayMap Bravo platform, offers an important methodological advancement for future studies seeking to investigate phosphorylated aSyn biomarkers in PD. Generating peptides is essential due to their smaller size that can be more easily handled and analyzed for MS analysis, which enables more accurate protein quantification and improves analytical reproducibility (Saveliev et al., 2013). We determined that the binding buffer with a concentration of 0.5% GA had the greatest percent enrichment (73.2%) and the largest quantity of STY peptides (17,864) among samples tested, surpassing those of 0%, 0.2%, 1%, and 2% GA (Figure 3A). The 0.5% GA binding buffer did not have the greatest amount of total peptides in comparison to other GA concentrations (0%, 0.2%, 2% GA), but it did demonstrate a high quantity of STY peptides relative to its total peptides, signifying specific binding and successful enrichment (Figure 3B). GA in the binding buffer has been shown to be more selective for phosphopeptides and reduces non-specific binding (Hernandez-Valladares et al., 2013); however, no GA addition was mentioned in the original protocol for Fe-NTA phosphoenrichment via AssayMap Bravo (Russell and Murphy, 2015). Therefore, this discovery is novel and provides valuable insights for future studies aiming to phosphoenrich their samples. Such advancements are expected to result in reduced sample complexity, increased detection specificity, and improved sensitivity, thereby enhancing the overall efficacy of phosphoproteomic analyses.

The elution buffer for phosphoenrichment of digested frontal cortex brain samples was then optimized with the addition of acetonitrile (ACN) to 1% NH<sub>4</sub>OH. ACN was added because it is an organic solvent that assists in the elution of hydrophobic proteins such as aSyn, our target protein. We determined that the optimal elution buffer concentration was 10% ACN, as it

resulted in the highest percent enrichment (89%) and a substantial quantity of STY peptides (6,519) compared to other tested concentrations (Figure 4A). Although 50% ACN also achieved an 89% enrichment and had a greater number of STY peptides (7,368) than 10% ACN, the total peptide and STY peptide counts were comparable between the two conditions (Figure 4B). Therefore, we selected 10% ACN as the optimal concentration since it required significantly less ACN while yielding similar results. ACN has been shown to reduce non-specific hydrophobic interactions during phosphopeptide enrichment and enable better identification of less abundant phosphopeptides (Fila and Honys, 2011). Yet, no ACN addition to the elution buffer was present in the original protocol for Fe-NTA phosphoenrichment via AssayMap Bravo (Russell and Murphy, 2015). Thus, our addition of ACN to the elution buffer helps to provide a more effective protocol for future investigations interested in phosphoproteomic analysis of RBCs.

Previous studies have demonstrated that TiO<sub>2</sub> exhibits selectivity for approximately 50% different phosphopeptides compared to Fe-NTA (ThermoFisher Scientific, 2024). In this study, we evaluated both techniques to determine their efficacy in discovering aSyn phosphorylation sites. We found that Fe-NTA identified 46% unique phosphopeptides, while TiO<sub>2</sub> identified 18.7%. Additionally, 33.3% of phosphopeptides were shared between the two techniques (Figure 5C). These findings diverge from previous research, suggesting that Fe-NTA enriches for a higher proportion (79.3%) of total phosphopeptides than TiO<sub>2</sub>. Consequently, Fe-NTA was identified as the preferred phosphoenrichment technique for analyzing erythrocyte ghost membranes moving forward.

After optimizing the phosphoenrichment protocol on the Bravo, we next needed to optimize the erythrocyte ghost membrane sample load. We found that 100 µg of erythrocyte ghost membrane sample was ideal, as it yielded the highest quantity of STY peptides (894) and

achieved a phosphoenrichment of 94.3% (Figure 6A). Moreover, the 100  $\mu$ g sample revealed the presence of the new phosphorylation site S87, in addition to the previously documented sites Y125 and S129, which were not detected in the other sample loads (Figure 7E). Validating this optimization of sample load for erythrocyte ghost membranes opens avenues for further research on RBC aSyn phosphorylation site biomarkers by establishing a framework that other scientists can use to reliably replicate findings.

There are no previous studies investigating erythrocyte aSyn phosphorylation sites using ghost membranes. This study demonstrates the presence of phosphorylated aSyn in erythrocyte ghost membranes. This was accomplished with the use of representative chromatographic peaks that indicate the presence of pY125, pS87, and pS129, respectively. In mass spectrometry, sharp chromatographic peaks indicate high resolution and a single analyte, which suggests high sensitivity of detection. In Figure 7C, we see relatively sharp peaks that include all 3 precursor ions as shown by the light green, blue, and purple peaks. These precursor ions are important in identifying and characterizing molecules in complex samples, and when they align in the chromatogram it enhances confidence in the identification of the analyte. The representative chromatogram for pY125 shows a pointed peak for the first precursor, a jagged peak for the second precursor, and a dull peak for the third precursor. Overall, it is a decent peak because the precursors are relatively lined up and distinct from one another. The pS87 peak has a sharp peak for the first precursor, a singular slightly rounded but still pointed peak for the second precursor, and a dull but slightly pointed peak for the third precursor. The pS129 peak is pointed for the first precursor, rounded base and sharp end peak for the second precursor, and a flat peak for the third precursor. Overall, each chromatogram instills confidence that the phosphorylation site of aSyn is present; however, the pS87 peak is the most representative of an ideal peak due to its

shape.

The x-axis of the chromatograms for figure 7C is the retention time, which represents the time it takes for a compound to elute from the chromatography column and reach the detector of the MS. The retention time is responsible for providing compound identification via peptide hydrophobic characteristics. Each representative chromatogram in this case has a retention time at around the 12.82-12.85 minute range, which is indicative of a consistency that is required for accurate identification of compounds by providing a characteristic elution pattern. The y-axis of the graph is the relative intensity of the peaks, which refers to the magnitude of the ion signal. When there is high intensity, it indicates that a large number of ions of a specific compound has been detected by MS. In the chromatogram for pY125, the intensity is relatively high with  $\sim 21 \cdot 10^3$  relative intensity. The same is seen in pS87, with a relative intensity of  $\sim 31 \cdot 10^3$ . However, in pS129 the relative intensity is quite low at 8,000. This means that aSyn pS129 has relatively low abundance in the sample, which does have implications in the reliability of pS129's presence that needs to be evaluated further. This is accomplished by the ion mobiligram.

Ion mobiligrams are plots that display the mobility of ions in gasses under the influence of an electric field, with the  $m/z$  ratio as the x-axis and ion mobility as the y-axis. The ion mobility is represented by  $1/K_0$ , which is the inverse of the ion's reduced mobility (Dodds and Baker, 2019). Reduced mobility is a measure of how quickly an ion moves in an electric field, which depends on the ion's size, charge and shape (Fernández-Maestre et al., 2010). The inverse is used because it is directly proportional to the collision cross-section of the ion, which is a physicochemical property known to depend on the shape and size of the ion (Wisnapiyakorn et al., 2024). Therefore, by using the  $1/K_0$ , it is a more straightforward comparison of the ions based on structural characteristics that help with identification. Within the mobiligram, you will also

see labels M+1 and M+2. The most abundant ion in the sample being the largest peak with the highest intensity is the M peak. The M+1 and the M+2 peak are both smaller peaks that correspond to an isotope of a compound that are one or two mass units greater than M. Being able to distinguish between isotopic peaks becomes crucial for biomarker discovery since molecules have distinct mass profiles due to variations caused by post-translational modifications and molecular structures.

In Figure 7D, a substantial number of dots fall within a defined ion mobility window, indicating the presence of ions of interest from the peaks in Figure 7C without interference from other ion species. Darker orange/red dots denote higher intensity, which are desirable for confirming the presence of an ion species. The ion mobiligram for pY125 and pS87 exhibits numerous dark orange/red dots within the ion mobility window, which instills confidence in the presence of peptides containing the phosphorylation sites. Although the ion mobiligram for pS129 is well-defined within the ion mobility window, there are fewer dark warm colors. This aligns with the relatively low intensity observed in Figure 7C. Nonetheless, the distinct peak shape and presence of a single ion species within the ion mobility window suggest that pS129 is indeed present in the erythrocyte ghost membrane sample.

Fragmentation spectra (MS/MS) depict the fragmentation patterns of ions, with the mass-to-charge ratio ( $m/z$ ) on the x-axis and intensity (%) on the y-axis. In Figure 7E, the peptide sequence and its corresponding phosphorylation PTM are displayed above the spectra. Green and orange lines represent b and y ions, respectively, where b ions are formed by cleaving peptide bonds at the N-terminal side of amino acid residues, and y ions are formed by cleaving peptide bonds at the C-terminal side. Identification of these ions enables researchers to determine the peptide sequence and detect PTMs like phosphorylation (Cleveland and Rose, 2013).

In the first fragmentation spectra, the presence of the b23 ion indicates pY125. Unlike chromatograms and ion mobiligrams, the b23 ion's presence containing the pY125 site is sufficient confirmation of the phosphorylation site's presence, whereas chromatograms and mobiligrams serve as levels of confidence (Figure 7E). In the second fragmentation spectra, pS87 is evidenced by multiple ions, including b15, b13, b9, b8, b7, y10, y11, y12, y13, y14, and y15. The y13 ion in the third fragmentation spectra is indicative of pS129 (Figure 7E). Therefore, we can say that there is evidence of the presence of Y125, S87, and S129 aSyn phosphorylation sites within erythrocyte ghost membranes.

This is the first study that has observed the phosphorylation site of S87 in erythrocyte aSyn. S87 is well documented as a phosphorylation site in the brain and is known to play an important role in aSyn aggregation and Lewy body formation (Oueslati et al., 2012; Paleologou et al., 2010; Zhang et al., 2023; Xu et al., 2015). Increased levels of pS87 are said to occur in vivo and are known to increase the amplification of Lewy body aSyn, which is a primary contributor to PD development (Zhang et al., 2023; Paleologou et al., 2010). Thus, it is noteworthy that our investigation not only revealed the presence of phosphorylated aSyn within erythrocyte ghost membranes, but that it also unveiled a novel, prominent phosphorylation site in red blood cells. The discovery of pS87 in erythrocytes could have major implications in future studies as a diagnostic biomarker for distinguishing the presence or absence of PD.

Furthermore, the study validated previous findings showing the presence of the phosphorylation sites of Y125 and S129 in erythrocyte aSyn. Phosphorylated Y125 (pY125) is hypothesized to play a neuroprotective role and prevent neurotoxicity caused by aSyn fibrils in PD (Xu et al., 2015). However, pY125 was also found to increase the binding affinity to Cu(II), Pb(II), and Fe(II), which are transition metals that are known to be involved in the pathogenesis

of synucleinopathies and aSyn toxicity (Lu et al., 2011). Therefore, more studies investigating the role of pY125 are needed to further understand its impact on PD pathogenesis. With the discovery of its presence in erythrocyte ghost membranes, blood could serve as a biospecimen to provide further clarity on aSyn pY125's role in PD.

Phosphorylation of S129 in aSyn is postulated to expedite the conversion from aSyn monomers to oligomeric, fibrillar forms, which are neurotoxic (Yamada et al., 2004). Additionally, pS129 has been demonstrated to markedly potentiate aSyn toxicity in dopaminergic neurons in *Drosophila* models (Chen and Feany, 2005). While the prevailing consensus implicates pS129 in Lewy body formation and dopaminergic neurodegeneration, conflicting evidence suggests a potential neuroprotective role or lack of affect altogether (Xu et al., 2015). Similar to pY125, further investigation is warranted to elucidate the precise role of pS129 in PD pathology, which is a pursuit that can be facilitated through the utilization of erythrocyte ghost membranes, as demonstrated in this study.

A limitation of this study pertains to the AssayMap Bravo method development, which was initially optimized using digested frontal cortex brain samples and subsequently applied without modifications to erythrocyte ghost membranes. The decision to utilize brain samples was driven by their relative abundance compared to the limited quantity of erythrocyte ghost membranes available for phosphoenrichment, necessitated by the labor-intensive process of ghost membrane production (0.5 - 1.0 mg). Although employing a single protocol across different sample types is feasible, it may not consistently yield optimal outcomes due to variations in tissue structure, cellular composition, protein stability, and post-translational modifications. Therefore, future investigations involving erythrocyte ghost membranes should consider evaluating the optimal concentrations of GA in the binding buffer and ACN in the

elution buffer to ensure robust and reproducible results.

This same limitation is also applicable with the Fe-NTA and TiO<sub>2</sub> phosphoenrichment technique comparison since a brain sample was also used in this instance. Erythrocyte ghost membranes could potentially have different unique phosphopeptide percentages in comparison to the brain, and thus it may be beneficial to do a comparison of the two phosphoenrichment techniques on erythrocyte ghost membranes for future studies to know which method best captures aSyn phosphorylation sites. There are also studies suggesting that the use of both IMAC and OMAC in combination with one another increases phosphoenrichment to >90%, which is called sequential enrichment by metal oxide affinity chromatography (SMOAC) (Jones et al., 2020). This technique could also be useful in future studies that assess and select for aSyn phosphorylation in erythrocyte ghost membranes.

This study presents a new methodological approach for optimizing the phosphoenrichment of digested frontal cortex brain samples by using advanced technology such as the Agilent AssayMap Bravo platform, which is a significant advancement for future investigations into phosphorylated aSyn biomarkers in PD. It also marks the first instance of employing MS with a DDA approach in conjunction with proteomic analysis software to identify aSyn phosphorylation sites within erythrocyte ghost membranes. This method surpasses the limitations of previous immunoassays for RBCs, which were constrained by antibody specificity. Furthermore, the novel identification of pS87 in erythrocytes could pave the way for investigations examining pS87 as a potential biomarker for early, non-invasive PD diagnosis.

### Future Directions

Future directions include developing a targeted MS-based proteomics assay for the precise quantification of analytes. A sensitive assay that could be used to quantify analytes to show that phosphorylated aSyn in RBCs can be an effective biomarker is selective reaction monitoring (SRM), which is also known as multiple reaction monitoring (MRM) and interchangeable depending on instrument vendor. SRM/MRM is a highly selective and sensitive analytical technique used in MS for the quantification and identification of low abundant proteins in complex mixtures as well as the characterization of modified peptides (Calvo et al., 2011). SRM/MRM is a valuable tool for validating clinical biomarkers, which is made possible by a readily available and economical instrument known as the triple quadrupole mass spectrometer (QQQ-MS). The triple quadrupole MS operates by precisely separating and measuring the masses of ions, which allows for the discernment of the molecules present within a given sample. It accomplishes this by using mass filters in the first and third quadrupole rods that specifically select for precursor peptide ions and product ions with predetermined mass-to-charge ratios. The second quadrupole rod acts as a collision cell that breaks down the selected ions (Creative Proteomics, 2023). These steps ensure the high selectivity of the SRM/MRM technique.

Another increased sensitive assay that could accomplish this goal is parallel reaction monitoring (PRM), which is made possible by the Orbitrap and TOF mass spectrometers. PRM is a high resolution, highly specific method for quantification of proteins of interest. For example, PRM with an Orbitrap-based mass spectrometer does this by selecting a precursor ion in the quadrupole that is then directed to the higher energy collision-induced dissociation cell for fragmentation via the collision cell. The fragment ions then return to the C-trap from the HCD

cell to be analyzed in the Orbitrap analyzer (Rauniyar, 2015). Of particular interest, both SRM/MRM and PRM can use heavy isotope synthetic peptides as an internal standard to quantify PTMs such as phosphorylation (Rauniyar, 2015). Using a calibration curve with the SRM or PRM acquisition methods allows us to make these absolute quantifications.

This curve enables the comparison of concentrations of aSyn phosphopeptides in the erythrocytes of PD patients versus those of healthy controls. The implementation of heavy isotope standards could facilitate the creation of a calibration curve. Heavy isotope standards, chemically identical to the target analytes but featuring isotopic labels such as C14 and N15, would serve as reference compounds during analysis (Borland et al., 2019). By measuring the ratio of peak intensities between labeled and unlabeled analytes in the mass spectrum, absolute quantification of the target analyte concentration relative to chromatogram intensity would become achievable.

After a calibration curve and concentrations are determined, it would then be important to calculate the receiver operating characteristic (ROC) curve to assess the diagnostic validity of the potential biomarker. ROCs help to identify the sensitivity and specificity of the biomarker according to the percentage of true positives and true negatives (English et al., 2016). For example, if pS129 was statistically significant in PD patients, it could be a false positive, which would be detected by the ROC curve. Therefore, future studies assessing erythrocyte aSyn phosphorylation sites as potential biomarkers in PD should use ROC curves to assess the accuracy of the diagnostic test.

## References

- 1) Agilent (2023) *AssayMAP Bravo Protein Sample Prep Platform*, Agilent. Available at: <https://www.agilent.com/en/product/automated-liquid-handling/automated-liquid-handling-applications/assaymap-bravo-protein-sample-prep-platform> (Accessed: 29 September 2023).
- 2) Arawaka, S., Sato, H., Sasaki, A. *et al.* Mechanisms underlying extensive Ser129-phosphorylation in  $\alpha$ -synuclein aggregates. *acta neuropathol commun* 5, 48 (2017). <https://doi.org/10.1186/s40478-017-0452-6>
- 3) Beeton-Kempen, Natasha. “Data-Dependent vs. Data-Independent Proteomic Analysis.” *Proteomics & Metabolomics from Technology Networks*, Apr. 2021, [www.technologynetworks.com/proteomics/lists/data-dependent-vs-data-independent-proteomic-analysis-331712](http://www.technologynetworks.com/proteomics/lists/data-dependent-vs-data-independent-proteomic-analysis-331712).
- 4) Borland, Kayla, et al. “Production and application of stable isotope-labeled internal standards for RNA modification analysis.” *Genes*, vol. 10, no. 1, 5 Jan. 2019, p. 26, <https://doi.org/10.3390/genes10010026>.
- 5) Califf, R.M. (2018) ‘Biomarker definitions and their applications’, *Experimental Biology and Medicine*, 243(3), pp. 213–221. doi:10.1177/1535370217750088.
- 6) Calvo, E. *et al.* (2011) ‘Applying selected reaction monitoring to targeted proteomics’, *Expert Review of Proteomics*, 8(2), pp. 165–173. doi:10.1586/epr.11.11.
- 7) Cariulo, C. *et al.* (2019) ‘Phospho-S129 alpha-synuclein is present in human plasma but not in cerebrospinal fluid as determined by an ultrasensitive immunoassay’, *Frontiers in Neuroscience*, 13. doi:10.3389/fnins.2019.00889.
- 8) Chen, Li, and Mel B Feany. “A-synuclein phosphorylation controls neurotoxicity and inclusion formation in a drosophila model of parkinson disease.” *Nature Neuroscience*, vol. 8, no. 5, 17 Apr. 2005, pp. 657–663, <https://doi.org/10.1038/nn1443>
- 9) Cleveland, James P, and John R Rose. “Identification of B-/Y-ions in MS/MS spectra using a two stage neural network.” *Proteome Science*, vol. 11, no. Suppl 1, 2013, <https://doi.org/10.1186/1477-5956-11-s1-s4>.
- 10) Connolly, B.S. and Lang, A.E. (2014) ‘Pharmacological treatment of parkinson disease’, *JAMA*, 311(16), p. 1670. doi:10.1001/jama.2014.3654.
- 11) Constantinides, V.C. *et al.* (2021) ‘Cerebrospinal fluid  $\alpha$ -synuclein species in cognitive and movements disorders’, *Brain Sciences*, 11(1), p. 119. doi:10.3390/brainsci11010119.

- 12) Dodds, James N., and Erin S. Baker. “Ion Mobility Spectrometry: Fundamental Concepts, instrumentation, applications, and The road ahead.” *Journal of the American Society for Mass Spectrometry*, vol. 30, no. 11, 6 Sept. 2019, pp. 2185–2195, <https://doi.org/10.1007/s13361-019-02288-2>.
- 13) El Turk, F. *et al.* (2018) ‘Exploring the role of post-translational modifications in regulating  $\alpha$ -synuclein interactions by studying the effects of phosphorylation on nanobody binding’, *Protein Science*, 27(7), pp. 1262–1274. doi:10.1002/pro.3412. Foulds, P.G. *et al.* (2011) ‘Phosphorylated  $\alpha$ -synuclein can be detected in blood plasma and is potentially a useful biomarker for parkinson’s disease’, *The FASEB Journal*, 25(12), pp. 4127–4137. doi:10.1096/fj.10-179192.
- 14) Ellis, Kathryn A, et al. “The Australian imaging, biomarkers and lifestyle (AIBL) study of aging: Methodology and baseline characteristics of 1112 individuals recruited for a longitudinal study of Alzheimer's disease.” *International Psychogeriatrics*, vol. 21, no. 4, Aug. 2009, pp. 672–687, <https://doi.org/10.1017/s1041610209009405>.
- 15) English, Patricia A, et al. “A case for the use of receiver operating characteristic analysis of potential clinical efficacy biomarkers in advanced renal cell carcinoma.” *Future Oncology*, vol. 12, no. 2, Jan. 2016, pp. 175–182, <https://doi.org/10.2217/fon.15.290>.
- 16) Estaun-Panzano, Juan, et al. “Monitoring  $\alpha$ -synuclein aggregation.” *Neurobiology of Disease*, vol. 176, Jan. 2023, p. 105966, <https://doi.org/10.1016/j.nbd.2022.105966>.
- 17) Fernández-Maestre, Roberto, et al. “Chemical standards in Ion Mobility Spectrometry.” *The Analyst*, vol. 135, no. 6, 2010, p. 1433, <https://doi.org/10.1039/b915202d>.
- 18) Fíla, Jan, and David Honys. “Enrichment techniques employed in phosphoproteomics.” *Amino Acids*, vol. 43, no. 3, 15 Oct. 2011, pp. 1025–1047, <https://doi.org/10.1007/s00726-011-1111-z>.
- 19) Foulds, P.G. *et al.* (2013) ‘A longitudinal study on  $\alpha$ -synuclein in blood plasma as a biomarker for parkinson’s disease’, *Scientific Reports*, 3(1). doi:10.1038/srep02540.
- 20) Fujiwara, Hideo, et al. “ $\alpha$ -Synuclein is phosphorylated in synucleinopathy lesions.” *Nature Cell Biology*, vol. 4, no. 2, 28 Jan. 2002, pp. 160–164, <https://doi.org/10.1038/ncb748>.
- 21) Fye, Haddy K., et al. “A robust mass spectrometry method for rapid profiling of erythrocyte ghost membrane proteomes.” *Clinical Proteomics*, vol. 15, no. 1, 21 Mar. 2018, <https://doi.org/10.1186/s12014-018-9190-4>.
- 22) Garg, Eshita, and Muhammad Zubair. “Mass Spectrometer.” *National Library of Medicine*, U.S. National Library of Medicine, 21 Jan. 2023, [www.ncbi.nlm.nih.gov/books/NBK589702/](http://www.ncbi.nlm.nih.gov/books/NBK589702/).

- 23) Group, B.S. (2023) *Remove hemoglobin from erythrocyte and whole blood lysates with Hemovoid™*, [www.biotechsupportgroup.com](http://www.biotechsupportgroup.com). Available at: <https://www.biotechsupportgroup.com/HemoVoid-Hemoglobin-Depletion-From-Erythrocytes-p/hvk.htm> (Accessed: 29 September 2023).
- 24) Haider, Ali. “Lewy Body Dementia.” *StatPearls [Internet]*., U.S. National Library of Medicine, 12 Feb. 2023, [www.ncbi.nlm.nih.gov/books/NBK482441/](http://www.ncbi.nlm.nih.gov/books/NBK482441/).
- 25) He, Tianen, et al. “Comparative evaluation of Proteome Discoverer and FragPipe for the TMT-based proteome quantification.” *Journal of Proteome Research*, vol. 21, no. 12, 31 Oct. 2022, pp. 3007–3015, <https://doi.org/10.1021/acs.jproteome.2c00390>.
- 26) Hernandez-Valladares, Maria, et al. “Quantitative proteomic analysis of compartmentalized signaling networks.” *Methods in Enzymology*, 2014, pp. 309–325, <https://doi.org/10.1016/b978-0-12-397925-4.00018-3>.
- 27) Jones, Andrew W., et al. “Assessing budding yeast phosphoproteome dynamics in a time-resolved manner using TMT10PLEX mass tag labeling.” *STAR Protocols*, vol. 1, no. 1, June 2020, p. 100022, <https://doi.org/10.1016/j.xpro.2020.100022>.
- 28) Kalia, L.V. (2019) ‘Diagnostic biomarkers for parkinson’s disease: Focus on  $\alpha$ -synuclein in cerebrospinal fluid’, *Parkinsonism & Related Disorders*, 59, pp. 21–25. doi:10.1016/j.parkreldis.2018.11.016.
- 29) Kawahata, Ichiro, et al. “Pathogenic impact of  $\alpha$ -synuclein phosphorylation and its kinases in  $\alpha$ -synucleinopathies.” *International Journal of Molecular Sciences*, vol. 23, no. 11, 1 June 2022, p. 6216, <https://doi.org/10.3390/ijms23116216>.
- 30) Klatt, Stephan, et al. “Optimizing red blood cell protein extraction for biomarker quantitation with Mass Spectrometry.” *Analytical and Bioanalytical Chemistry*, vol. 412, no. 8, 6 Feb. 2020, pp. 1879–1892, <https://doi.org/10.1007/s00216-020-02439-5>.
- 31) Li, X.-Y. *et al.* (2021) ‘Alterations of erythrocytic phosphorylated alpha-synuclein in different subtypes and stages of parkinson’s disease’, *Frontiers in Aging Neuroscience*, 13. doi:10.3389/fnagi.2021.623977.
- 32) Lin, C.-H. *et al.* (2019) ‘Plasma PS129- $\alpha$ -synuclein is a surrogate biofluid marker of motor severity and progression in parkinson’s disease’, *Journal of Clinical Medicine*, 8(10), p. 1601. doi:10.3390/jcm8101601.
- 33) Lu, Yu, et al. “Phosphorylation of  $\alpha$ -synuclein at Y125 and S129 alters its metal binding properties: Implications for understanding the role of  $\alpha$ -synuclein in the pathogenesis of

- parkinson's disease and related disorders." *ACS Chemical Neuroscience*, vol. 2, no. 11, 30 Sept. 2011, pp. 667–675, <https://doi.org/10.1021/cn200074d>.
- 34) Mahul-Mellier, A.-L. *et al.* (2014) 'C-ABL phosphorylates  $\alpha$ -synuclein and regulates its degradation: Implication for  $\alpha$ -synuclein clearance and contribution to the pathogenesis of parkinson's disease', *Human Molecular Genetics*, 23(11), pp. 2858–2879. doi:10.1093/hmg/ddt674.
- 35) Manzanza, N. de, Sedlackova, L. and Kalaria, R.N. (2021) 'Alpha-synuclein post-translational modifications: Implications for pathogenesis of lewy body disorders', *Frontiers in Aging Neuroscience*, 13. doi:10.3389/fnagi.2021.690293.
- 36) Mohandas, Narla, and Patrick G. Gallagher. "Red Cell Membrane: Past, present, and future." *Blood*, vol. 112, no. 10, 15 Nov. 2008, pp. 3939–3948, <https://doi.org/10.1182/blood-2008-07-161166>.
- 37) Nemani, V.M. *et al.* (2010) 'Increased expression of  $\alpha$ -synuclein reduces neurotransmitter release by inhibiting synaptic vesicle reclustering after endocytosis', *Neuron*, 65(1), pp. 66–79. doi:10.1016/j.neuron.2009.12.023.
- 38) Ohlsson, Claes, et al. "Comparisons of immunoassay and mass spectrometry measurements of serum estradiol levels and their influence on Clinical Association Studies in men." *The Journal of Clinical Endocrinology & Metabolism*, vol. 98, no. 6, 1 June 2013, <https://doi.org/10.1210/jc.2012-3861>.
- 39) Oliveira Manzanza, Nelson De, et al. "Alpha-synuclein post-translational modifications: Implications for pathogenesis of lewy body disorders." *Frontiers in Aging Neuroscience*, vol. 13, 25 June 2021, <https://doi.org/10.3389/fnagi.2021.690293>.
- 40) Oueslati, Abid, et al. "Mimicking phosphorylation at serine 87 inhibits the aggregation of human  $\alpha$ -synuclein and protects against its toxicity in a rat model of parkinson's disease." *The Journal of Neuroscience*, vol. 32, no. 5, 1 Feb. 2012, pp. 1536–1544, <https://doi.org/10.1523/jneurosci.3784-11.2012>.
- 41) Paleologou, Katerina E., et al. "Phosphorylation at S87 is enhanced in synucleinopathies, inhibits  $\alpha$ -synuclein oligomerization, and influences Synuclein-membrane interactions." *The Journal of Neuroscience*, vol. 30, no. 9, 3 Mar. 2010, pp. 3184–3198, <https://doi.org/10.1523/jneurosci.5922-09.2010>.

- 42) Pino, Lindsay K., et al. "The Skyline Ecosystem: Informatics for Quantitative Mass Spectrometry Proteomics." *Mass Spectrometry Reviews*, vol. 39, no. 3, 9 July 2017, pp. 229–244, <https://doi.org/10.1002/mas.21540>.
- 43) Proteomics, C. (2023) *Introduction on selected / multiple reaction monitoring and parallel reaction monitoring*, *Creative Proteomics*. Available at: <https://www.creative-proteomics.com/resource/selected-multiple-reaction-and-parallel-reaction-monitoring.htm> (Accessed: 29 September 2023).
- 44) Rauniyar, Navin. "Parallel Reaction Monitoring: A targeted experiment performed using high resolution and high mass accuracy mass spectrometry." *International Journal of Molecular Sciences*, vol. 16, no. 12, 2 Dec. 2015, pp. 28566–28581, <https://doi.org/10.3390/ijms161226120>.
- 45) Roberts, Blaine R., et al. "Rubidium and potassium levels are altered in alzheimer's disease brain and blood but not in cerebrospinal fluid." *Acta Neuropathologica Communications*, vol. 4, no. 1, 14 Nov. 2016, <https://doi.org/10.1186/s40478-016-0390-8>.
- 46) Russell, Jason D., and Steve Murphy. "Agilent AssayMAP Bravo Technology Enables Reproducible Automated Phosphopeptide Enrichment from Complex Mixtures Using High-Capacity Fe(III)-NTA Cartridges." *Agilent*, Agilent Technologies, Inc, Mar. 2016, [www.agilent.com/cs/library/applications/5991-6073EN.pdf](http://www.agilent.com/cs/library/applications/5991-6073EN.pdf).
- 47) Samuel, Filsy, et al. "Effects of serine 129 phosphorylation on  $\alpha$ -synuclein aggregation, Membrane Association, and Internalization." *Journal of Biological Chemistry*, vol. 291, no. 9, Feb. 2016, pp. 4374–4385, <https://doi.org/10.1074/jbc.m115.705095>.
- 48) Saveliev, Sergei, et al. "Trypsin/Lys-C protease mix for enhanced protein mass spectrometry analysis." *Nature Methods*, vol. 10, no. 11, 30 Oct. 2013, pp. i–ii, <https://doi.org/10.1038/nmeth.f.371>.
- 49) Schultz, W. (2007) 'Behavioral dopamine signals', *Trends in Neurosciences*, 30(5), pp. 203–210. doi:10.1016/j.tins.2007.03.007.
- 50) Scientific, Thermo Fisher. "Peptide Enrichment and Fractionation." Thermo Fisher Scientific, 2024.
- 51) Sobsey CA, Ibrahim S, Richard VR, Gaspar V, Mitsa G, Lacasse V, Zahedi RP, Batist G, Borchers CH. Targeted and Untargeted Proteomics Approaches in Biomarker Development. *Proteomics*. 2020 May;20(9):e1900029. doi: 10.1002/pmic.201900029. Epub 2020 Jan 30. PMID: 31729135.

- 52) Spillantini, Maria Grazia, et al. "A-synuclein in Lewy bodies." *Nature*, vol. 388, no. 6645, 28 Aug. 1997, pp. 839–840, <https://doi.org/10.1038/42166>.
- 53) Sturgeon, Catharine M, and Adie Viljoen. "Analytical error and interference in immunoassay: Minimizing risk." *Annals of Clinical Biochemistry: International Journal of Laboratory Medicine*, vol. 48, no. 5, 12 July 2011, pp. 418–432, <https://doi.org/10.1258/acb.2011.011073>.
- 54) Tajik, Mohammad, et al. "Single-cell mass spectrometry." *Trends in Biotechnology*, vol. 40, no. 11, Nov. 2022, pp. 1374–1392, <https://doi.org/10.1016/j.tibtech.2022.04.004>.
- 55) Thingholm, Tine E. and Martin R. Larsen. "Phosphopeptide enrichment by immobilized metal affinity chromatography." *Phospho-Proteomics*, 2016, pp. 123–133, [https://doi.org/10.1007/978-1-4939-3049-4\\_8](https://doi.org/10.1007/978-1-4939-3049-4_8).
- 56) Tian, C. *et al.* (2019) 'Erythrocytic  $\alpha$ -synuclein as a potential biomarker for parkinson's disease', *Translational Neurodegeneration*, 8(1). doi:10.1186/s40035-019-0155-y.
- 57) Tu, Hai-Yue, et al. "A-synuclein suppresses microglial autophagy and promotes neurodegeneration in a mouse model of parkinson's disease." *Aging Cell*, vol. 20, no. 12, 22 Nov. 2021, <https://doi.org/10.1111/acer.13522>.
- 58) Vicente Miranda, H. *et al.* (2017) 'Posttranslational modifications of blood-derived alpha-synuclein as biochemical markers for parkinson's disease', *Scientific Reports*, 7(1). doi:10.1038/s41598-017-14175-5.
- 59) Wang, Y. *et al.* (2012) 'Phosphorylated  $\alpha$ -synuclein in parkinson's disease', *Science Translational Medicine*, 4(121). doi:10.1126/scitranslmed.3002566.
- 60) Wisanpitayakorn, Pattipong, et al. "Accurate prediction of ion mobility collision cross-section using ion's polarizability and molecular mass with limited data." *Journal of Chemical Information and Modeling*, vol. 64, no. 5, 23 Feb. 2024, pp. 1533–1542, <https://doi.org/10.1021/acs.jcim.3c01491>.
- 61) Xu, Y., Deng, Y. and Qing, H. (2015) 'The phosphorylation of  $\alpha$ -synuclein: Development and implication for the mechanism and therapy of the parkinson's disease', *Journal of Neurochemistry*, 135(1), pp. 4–18. doi:10.1111/jnc.13234.
- 62) Yamada, Masanori, et al. "Overexpression of  $\alpha$ -synuclein in rat substantia nigra results in loss of dopaminergic neurons, phosphorylation of  $\alpha$ -synuclein and activation of caspase-9: Resemblance to pathogenetic changes in parkinson's disease." *Journal of Neurochemistry*, vol. 91, no. 2, 10 Sept. 2004, pp. 451–461, <https://doi.org/10.1111/j.1471-4159.2004.02728.x>.

- 63) Zhang, S. *et al.* (2023) 'Post-translational modifications of soluble  $\alpha$ -synuclein regulate the amplification of pathological  $\alpha$ -synuclein', *Nature Neuroscience*, 26(2), pp. 213–225. doi:10.1038/s41593-022-01239-7.